JACS
JOURNAL OF THE AMERICAN CHEMICAL SOCIETY

Communication

pubs.acs.org/JACS

Electrogenerated Chemiluminescence for Potentiometric Sensors

Gastón A. Crespo, Günter Mistlberger, and Eric Bakker*

Department of Inorganic, Analytical and Applied Chemistry, University of Geneva, Quai E.-Ansermet 30, CH-1211 Geneva, Switzerland

Supporting Information

ABSTRACT: We report here on a generic approach to read out potentiometric sensors with electrogenerated chemiluminescence (ECL). In a first example, a potassium ion-selective electrode acts as the reference electrode and is placed in contact with the sample solution. The working electrode of the three-electrode cell is responsible for ECL generation and placed in a detection solution containing tris(2,2′-bipyridyl)ruthenium(II) [$Ru(bpy)_3^{2+}$] and the coreactant 2-(dibutylamino)ethanol (DBAE), physically separated from the sample by a bridge. Changes in the sample potassium concentration directly modulate the potential at the working electrode, and hence the ECL output, when a constant-potential pulse is applied between the two electrodes. A linear response of the ECL intensity to the logarithmic potassium concentration between 10 μm and 10 mM was found.

We present here for the first time a generic approach for observing direct electrogenerated chemiluminescence (ECL) output for potentiometric ion sensors. ECL is an attractive technique that takes advantage of spectroscopic and electrochemical methodologies[1−3] and lends itself well to the design of hand-held sensing devices because the emitted light signal can be observed visually or with conventional cameras.[4]

The general concept introduced here couples the potential generated at the interface of the membrane with the ECL emission. Both the input (perturbation) and output (detection) signals are electrochemically generated, providing a basis for future approaches that would be difficult to achieve with traditional electronics, including the achievement of two-dimensional chemical detection based on imaging tools or arrays of bipolar electrodes with ECL.[5−7] This research draws also some analogy from enzyme logic systems pioneered by Katz, in which logical operations are performed directly at the chemical level to realize integrated sensing systems.[8]

Potentiometric ion sensors are today well-established tools in analytical chemistry and account for billions of measurements each year in clinical diagnostics, environmental sensing, and benchtop measurements.[9,10] Unfortunately, a direct optical readout for potentiometric sensors normally fails because concentration changes within the membrane are typically negligible within the linear response region of the membrane electrode.[11] Consequently, optical ion sensors operate either on the basis of classical indicator chemistry (embedded in a hydrogel phase)[12,13] or make use of competitive ion-exchange or coextraction equilibria involving lipophilic sensing phases containing selective receptors that are borrowed from their potentiometric counterparts.[14−16] While the former principle suffers from a limited choice of indicators, the latter always detects the concentration (strictly, activity) of two competing or cooperative ions.

Recent work in our group has demonstrated that the sample compartment can be spatially separated from that of ECL generation if a cation-exchanging liquid membrane is used that transports the ECL reagent $Ru(bpy)_3^{2+}$ from the sample to a thin-layer ECL compartment by electrochemical excitation.[17] However, it would be attractive to introduce a generic methodology to provide ECL readout for potentiometric sensors without the need to pass current across the ion-selective membrane.

Direct ECL readout of potentiometric sensors can be achieved in the arrangement shown in Figure 1. The potential

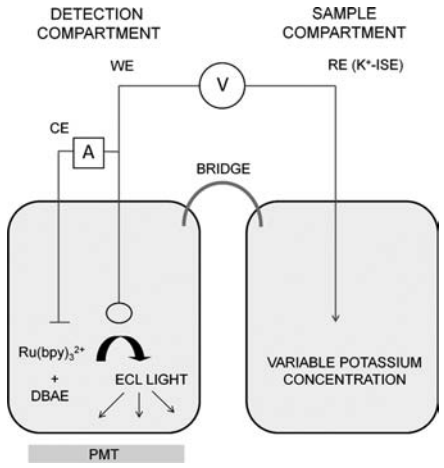

Figure 1. Schematic illustration of the electrochemical setup with two separated compartments (sample and detection) used to demonstrate the ECL readout concept for potentiometric sensors. An applied potential between the gold working electrode (WE) and the K^+ ISE reference electrode (RE) produces the oxidation of $Ru(bpy)_3^{2+}$ and 2-(dibutylamino)ethanol (DBAE), generating light at the gold electrode. The light is collected with a photomultiplier tube (PMT) placed outside the detection compartment. The reference potential is modulated by the activity of K^+ in the sample. The potassium ion-selective membrane is composed of a valinomycin-doped polymeric membrane (see the SI for membrane composition). The counter electrode (CE) is placed in the detection compartment.

Received: November 11, 2011
Published: December 15, 2011

is applied at the ECL-generating working electrode (WE) with respect to the reference electrode (RE), which is replaced here by the ion-selective electrode (ISE). This indicator electrode is in contact with the sample solution and physically separated from the location of ECL generation by a bridge. When a constant potential is applied across the cell, the potential at the ECL-generating WE directly depends on the potential at the ion-selective electrode. Ion activity changes in the sample may be monitored by ECL via the resulting potential change at the indicator electrode if the ECL intensity is potential-dependent.

A K^+ ISE was chosen as the indicator electrode in this early example. Figure 2A shows linear sweep voltammograms from 0 to 1.6 V for the setup illustrated in Figure 1 as a function of the K^+ concentration in the sample compartment. As established, the current flows between the WE and the counter electrode (CE) placed in the ECL compartment. The individual voltammograms are shifted along the potential axis according to the potential change at the indicator electrode. The potential separation agrees with the sample K^+ concentration according to the Nernst equation, with an observed slope of -58.3 ± 0.2 mV (the ideal value is -59.2 mV at 25 °C), as shown in the Figure 2A inset. The slope is negative because the indicator electrode assumes the position of the RE in the cell, resulting in a reversal of the sign of the potential. The detection limit observed in the inset is below 1 μM K^+ concentration, which is in accordance with other literature reports on similarly formulated membrane electrode systems.[18]

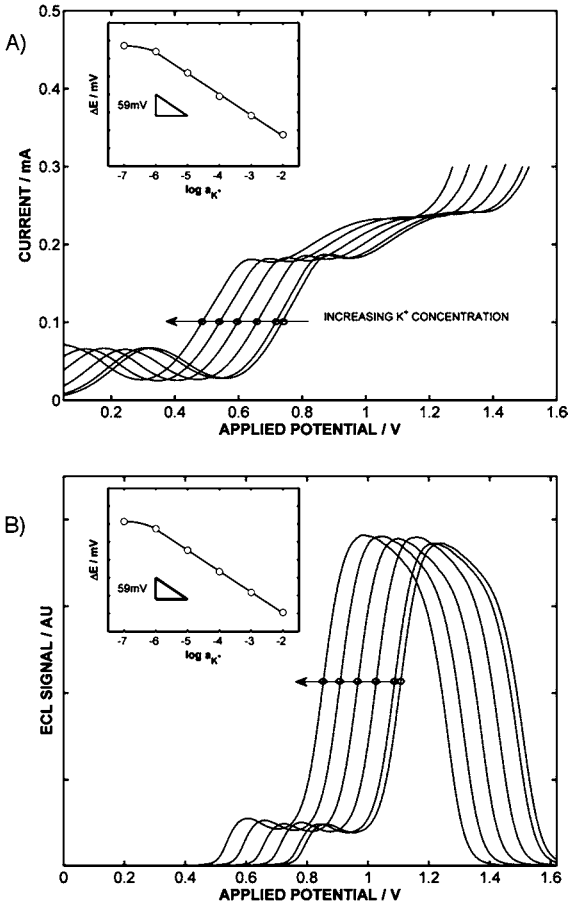

Figure 2. (A) Linear sweep voltammograms (current vs applied potential between the WE and RE) for the configuration shown in Figure 1. Increasing K^+ concentrations in a 10 mM LiCl background electrolyte shift the voltammograms to lower potentials. The arrow indicates the direction of increasing K^+ concentration (0.1 μM, 1 μM, 10 μM, 100 μM, 1 mM, and 10 mM, with sulfate as the counterion). Inset: Observed potential shift (ΔE) as a function of the logarithmic K^+ concentration for the current value indicated by the horizontal arrow in (A). (B) Corresponding ECL signal as a function of the linear sweep potential for different K^+ concentrations in the sample compartment. Inset: Observed Nernstian potential shift (ΔE) as a function of the logarithmic K^+ concentration for the ECL output indicated by the horizontal line in (B).

The first voltammetric peak at ~0.3 V is attributed to the oxidation of the coreactant 2-(dibutylamino)ethanol (DBAE) and does not result in ECL generation (also see refs 19 and 20). The second wave in the range of ~0.8−1.3 V generates an intense red light emission and is attributed to the concurrent oxidation of $Ru(bpy)_3^{2+}$ and DBAE[21] (see Figure 2B). When the K^+ concentration increases, the ECL peaks shift to less negative potentials, following the behavior of the current response shown in Figure 2A. The same magnitude of light output is observed for the individual measurements, but the shift is again a function of the K^+ concentration in the sample compartment with a near-Nernstian slope of -58.5 ± 0.3 mV.

The potentiometric characteristics of the K^+ ISE were evaluated separately with a high-impedance interface. A near-Nernstian slope of 59.7 ± 0.2 mV dec^{-1} with respect to K^+ was observed [see Figure 1S in the Supporting Information (SI)], in agreement with the potential shifts shown in Figure 2 under dynamic electrochemistry conditions. Unbiased selectivity coefficients were estimated with the modified separate solutions method.[22] The resulting values are shown in the SI and confirm that a high concentration of Li^+ on the order of 10 mM does not influence the potentiometric response (and hence the ECL output) in the chosen K^+ concentration range, with $\log K_{K,Li} = -6.6 \pm 0.1$. The lower limit of detection and the linear working range are shown in Figure 2S.

Having established that the potential at the WE can be modulated by the potential at the ISE, we subsequently demonstrated direct ECL detection of the K^+ concentration. According to the data in Figure 2B, the largest changes in ECL amplitude should be observed at a constant applied cell potential in the rising edge of the ECL-versus-potential spectrum (i.e., in the range of 0.8 to 1.0 V). Figure 3A demonstrates calibration curves for K^+ at three different applied potentials (0.8, 0.9, and 1 V). The experiments were performed by applying potential pulses of 0.1 s duration and collecting the emitted light at the WE with a photomultiplier tube. The maximum sensitivity was found for a potential of 1 V (see Figure 3A). While the data in Figure 2B suggest a roughly sigmoidal response function, a near-linear range from 50 μM to 10 mM K^+ concentration was observed (Figure 3A). The response at the lower potentials did not give obvious advantages (also see Figure 3S).

Rapid fixed potential pulses to generate ECL show promising reproducibility, as shown in Figure 3B. The low consumption of reagents during the short pulses reduces any significant attenuation of the ECL signal with time. Figure 3B shows the transient ECL signal at a 1 V applied potential as a function of the concentration of potassium in the sample compartment, demonstrating a relative standard deviation (RSD) of 0.3−0.5% in the ECL output.

In summary, this work has shown how a selective potentiometric sensor can be used to modulate the potential at a working electrode that is placed in a compartment

dx.doi.org/10.1021/ja210600k | J. Am. Chem.Soc. 2012, 134, 205−207

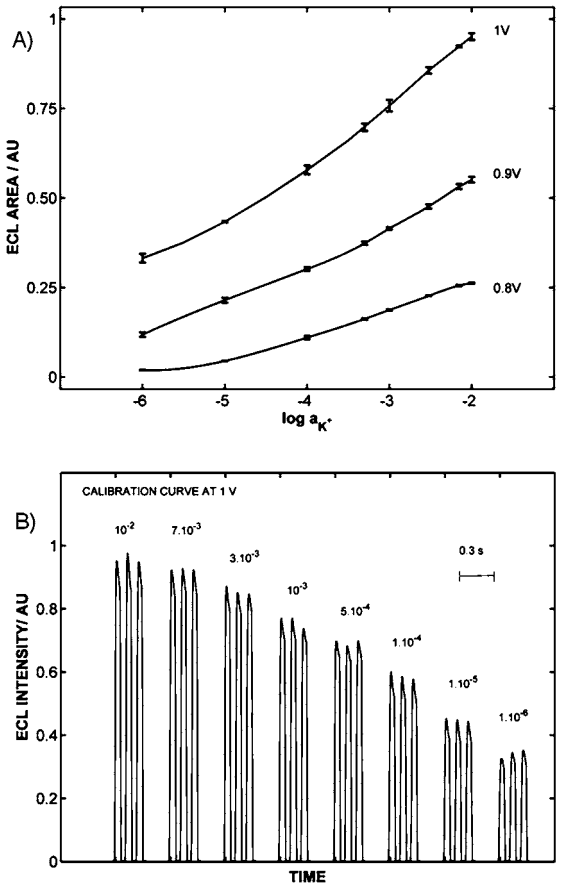

Figure 3. (A) ECL calibration curves for different K^+ levels at three external applied potentials: 0.8 V, 0.9 and 1 V. Error bars have been added for each potassium activity. (B) ECL peaks as a function of time recorded when short chronoamperometric pulses were applied on the cell. The peak width is 0.1 s, and the amplitude depends on the K^+ concentration. The reproducibility of the peak maxima (RSD < 2%, n = 3) is somewhat inferior to that for the integrated ECL peaks (error bars in Figure 2A).

optimized for efficient electrogenerated chemiluminescene detection. For the system explored here, a 1 V applied potential gives rise to large and reproducible changes in ECL intensity, demonstrating a generic approach to yield direct light emission readout for potentiometric sensors. The system introduced here relies on the potential of a second electrode placed in the sample compartment to close the cell circuit (in a final design most appropriately through a liquid junction). This means that an optical readout for ion concentration changes can now be accomplished for the first time with extra-thermodynamic assumptions that are no more severe than those for established ion-selective electrodes.

■ ASSOCIATED CONTENT

Ⓢ Supporting Information

Experimental details, potentiometric characterization, and ECL peaks at different applied potentials. This material is available free of charge via the Internet at http://pubs.acs.org.

■ AUTHOR INFORMATION

Corresponding Author

eric.bakker@unige.ch

■ ACKNOWLEDGMENTS

The authors thank the Swiss National Science Foundation and the University of Geneva for supporting this research. We also thank S. Jeanneret for electronics support.

■ REFERENCES

(1) Miao, W. J. *Chem. Rev.* **2008**, *108*, 2506−2553.
(2) Richter, M. M. *Chem. Rev.* **2004**, *104*, 3003−3036.
(3) Bard, A. J. *Electrogenerated Chemiluminescence*; Marcel Dekker: New York, 2004.
(4) Delaney, J. L.; Hogan, C. F.; Tian, J. F.; Shen, W. *Anal. Chem.* **2011**, *83*, 1300−1306.
(5) Chow, K. F.; Mavre, F.; Crooks, R. M. *J. Am. Chem. Soc.* **2008**, *130*, 7544−7545.
(6) Chow, K. F.; Mavre, F.; Crooks, J. A.; Chang, B. Y.; Crooks, R. M. *J. Am. Chem. Soc.* **2009**, *131*, 8364−8365.
(7) Mavre, F.; Anand, R. K.; Laws, D. R.; Chow, K. F.; Chang, B. Y.; Crooks, J. A.; Crooks, R. M. *Anal. Chem.* **2010**, *82*, 8766−8774.
(8) Katz, E.; Privman, V. *Chem. Soc. Rev.* **2010**, *39*, 1835−1857.
(9) Bakker, E.; Pretsch, E. *Angew. Chem., Int. Ed.* **2007**, *46*, 5660−5668.
(10) Pretsch, E. *TrAC, Trends Anal. Chem* **2007**, *26*, 46−51.
(11) Bakker, E.; Buhlmann, P.; Pretsch, E. *Chem. Rev.* **1997**, *97*, 3083−3132.
(12) Citterio, D.; Takeda, J.; Kosugi, M.; Hisamoto, H.; Sasaki, S.; Komatsu, H.; Suzuki, K. *Anal. Chem.* **2007**, *79*, 1237−1242.
(13) Clark, H. A.; Kopelman, R.; Tjalkens, R.; Philbert, M. A. *Anal. Chem.* **1999**, *71*, 4837−4843.
(14) Morf, W. E.; Seiler, K.; Rusterholz, B.; Simon, W. *Anal. Chem.* **1990**, *62*, 738−742.
(15) Suzuki, K.; Tohda, K.; Tanda, Y.; Ohzora, H.; Nishihama, S.; Inoue, H.; Shirai, T. *Anal. Chem.* **1989**, *61*, 382−384.
(16) Wolfbeis, O. S. *Anal. Chem.* **2008**, *80*, 4269−4283.
(17) Crespo, G. A.; Mistlberger, G.; Bakker, E. *Chem. Commun.* **2011**, *47*, 11644−11646.
(18) Bakker, E. *J. Electrochem. Soc.* **1996**, *143*, L83−L85.
(19) Zu, Y. B.; Bard, A. J. *Anal. Chem.* **2000**, *72*, 3223−3232.
(20) Zu, Y. B.; Bard, A. J. *Anal. Chem.* **2001**, *73*, 3960−3964.
(21) Liu, X. Q.; Shi, L. H.; Niu, W. X.; Li, H. J.; Xu, G. B. *Angew. Chem., Int. Ed.* **2007**, *46*, 421−424.
(22) Bakker, E.; Pretsch, E.; Buhlmann, P. *Anal. Chem.* **2000**, *72*, 1127−1133.